Nucleon resonances in the constituent quark model with chiral symmetry

H. Kowata, M. Arima
Department of Physics, Osaka City University, Osaka 558, Japan

K. Masutani
Faculty of Liberal Arts and Education, Yamanashi University, Kofu 400, Japan

Abstract

The mass spectra of nucleon resonances with spin $\frac{1}{2}$, $\frac{3}{2}$, and $\frac{5}{2}$ are systematically studied in the constituent quark model with meson-quark coupling, which is inspired by the spontaneous breaking of chiral symmetry of QCD. The meson-quark coupling gives rise not only to the one-meson-exchange potential between quarks but also to the self-energy of baryon resonances due to the existence of meson-baryon decay channels. The two contributions are consistently taken into account in the calculation. The gross properties of the nucleon resonance spectra are reproduced fairly well although the predicted mass of $N(1440)$ is too high.

11.30.Rd, 12.39.Jh, 14.20.Gk

1 Introduction

Although the constituent quark models have been successful in reproducing various static properties of baryons [1, 2], there still remains several problems. One of them is the mass spectrum of the spin $\frac{1}{2}$ nucleon resonances. The conventional models cannot explain the fact that the ground state is remarkably light while the separations among the excited states are relatively narrow [3]. Furthermore, the mass of $N(1440)$ is predicted to be too high.

Glozman *et al.* have recently examined baryon mass spectra by using the constituent quark model with the one-meson-exchange potential (OMEP) as the residual interaction between quarks [4, 5, 6], whereas the conventional models contain the one-gluon-exchange potential (OGEP) instead [7]. The OMEP has been introduced on the basis of the spontaneous breaking of chiral symmetry (SBχS) in low-energy QCD. In direct consequence of SBχS, there appear Nambu-Goldstone bosons (i.e., the flavor-octet pseudoscalar mesons such as π, K, and η) as well as the mass of light quarks [8, 9]. In addition to the flavor-octet mesons, the flavor-singlet η' has been also taken into account for the Nambu-Goldstone bosons. Glozman *et al.* have claimed that the model provides a unified description of the ground states and the excitation spectra of baryon resonances. They have also pointed out that the spin-flavor dependence of the OMEP is important to reproduce the mass spectra.

On the other hand, there exists another type of mesonic effects. The self-energy of baryons, which comes from the coupling between single baryon states and meson-baryon scattering states, have been studied by one of the authors (M.A.) and his collaborators [10, 11, 12]. They have shown, for example, that the large ηN decay width of $N(1535)$ as well as the mass splitting between $\Lambda(1405)$ and $\Lambda(1520)$ can be explained by the effect of the self-energy. We note here that they have used the OGEP for the residual quark-quark interaction.

In this paper, we construct the model consisting of the constituent quarks and the pseudoscalar mesons with the pseudovector meson-quark coupling. The quarks and mesons are treated as the elementary degrees of freedom on the basis of SBχS. Since the meson-quark coupling gives rise not only to the OMEP but also to the self-energy, the two mesonic effects can be treated on an equal footing. The OMEP mainly stems from the exchange of the off-energy-shell mesons whose energies are nearly equal to zero, while the self-energy does from the on-energy-shell mesons. The two contributions, however, cannot be strictly separated as is clearly seen in the relativistic formalism where they correspond to the same diagram [13]. Therefore, the problem of double counting should be resolved in order to treat them in a consistent manner. The purpose of this work is not to obtain a perfect fit to the observed baryon masses but to investigate the consistent model containing the two mesonic effects. We calculate the mass spectra of nucleon resonances and mainly examine the dynamical effect on the mass spectrum of the self-energy, which is absent in the conventional calculations. The self-energy provides the energy-dependent effect on resonance masses, while the OMEP does the static effect.

The paper is organized as follows. In Section 2, the constituent quark model with the meson-quark coupling is presented, and the OMEP and the self-energy are derived with an emphasis on the problem of double counting. The method of calculation is explained also. The numerical results for nucleon resonances are shown in Section 3. The summary of the paper is given in Section 4.

2 Model

The model Hamiltonian for the meson-quark system H consists of the internal Hamiltonian of the baryon H_0, the kinetic energy of the baryon T_B (i.e., the center-of-mass (c.m.) motion of the three quarks), the total energy of the meson ω_M, and the meson-quark coupling H_I, as follows:

$$H = H_0 + T_B + \omega_M + H_I \ , \tag{1}$$

with

$$H_0 = T_0 + V_{\rm conf} + M_0 \ , \tag{2}$$

where T_0 is the kinetic energy of the quarks without the c.m. motion, $V_{\rm conf}$ the confinement potential for the quarks, and M_0 the constant mass parameter of the baryon. Note that T_B and ω_M have non-vanishing contributions only for meson-baryon scattering channels.

The non-relativistic kinematics is used for the constituent quarks:

$$T_0 + T_B = \sum_{i=1}^{3} \frac{\boldsymbol{p}_i^2}{2m}, \tag{3}$$

where m is the quark mass and $\boldsymbol{p}_i$ the momentum of the ith quark. Here the mass difference between u- and d-quarks is neglected and the conventional value of the quark mass is used: $m = 340\,\mathrm{MeV}$. The above decomposition can be easily done by means of Jacobi coordinates in the non-relativistic kinematics. This property is quite favorable in the investigation of baryon mass spectra and meson-baryon scattering.

For the confinement potential that ensures the three quarks are always confined in the baryon, the linear form is employed:

$$V_{\text{conf}} = c \sum_{i<j}^{3} |\boldsymbol{r}_i - \boldsymbol{r}_j| \ , \tag{4}$$

where c is the strength parameter and $\boldsymbol{r}_i$ the coordinate of the ith quark. This type of confinement is suggested by the lattice QCD calculations for heavy quark systems [14] as well as by the flux tube model [15]. Since light constituent quarks are considered in this work, c should be treated as a phenomenological parameter. The bare mass M_0 is a free parameter also.

For the meson-quark coupling H_I, the non-relativistic form of the pseudovector coupling is employed:

$$\begin{aligned} H_I \ &= \ \sum_{i=1}^{3} \left\{ \frac{i g_{Mqq}}{2m} \rho(\boldsymbol{k}) \left[\frac{\omega_M}{2m} \left(\boldsymbol{\sigma}_i \cdot \overleftarrow{\boldsymbol{p}}_i \, \boldsymbol{\lambda}_i \cdot \boldsymbol{\phi}_i(\boldsymbol{k}) \right.\right.\right. \\ &\quad + \left. \boldsymbol{\lambda}_i \cdot \boldsymbol{\phi}_i(\boldsymbol{k}) \, \boldsymbol{\sigma}_i \cdot \overrightarrow{\boldsymbol{p}}_i \right) - \left. \boldsymbol{\sigma}_i \cdot \boldsymbol{k} \, \boldsymbol{\lambda}_i \cdot \boldsymbol{\phi}_i(\boldsymbol{k}) \right] \\ &\quad + \frac{i g_{\eta' qq}}{\sqrt{6} m} \rho(\boldsymbol{k}) \left[\frac{\omega_{\eta'}}{2m} \left(\boldsymbol{\sigma}_i \cdot \overleftarrow{p}_i \, \phi_i^{\eta'}(\boldsymbol{k}) + \phi_i^{\eta'}(\boldsymbol{k}) \, \boldsymbol{\sigma}_i \cdot \overrightarrow{p}_i \right) \right. \\ &\quad - \left.\left. \boldsymbol{\sigma}_i \cdot \boldsymbol{k} \, \phi_i^{\eta'}(\boldsymbol{k}) \right] \right\} + \text{h.c.} \ , \end{aligned} \tag{5}$$

with

$$\rho(\boldsymbol{k}) = \exp\left(-\frac{k^2}{8a^2} \right) \ , \tag{6}$$

$$\boldsymbol{\phi}_i(\boldsymbol{k}) = \frac{1}{\sqrt{2\omega_M}} \boldsymbol{a}_i(\boldsymbol{k}) \, e^{ik} \cdot \boldsymbol{r}_i \ , \tag{7}$$

$$\phi_i^{\eta'}(\boldsymbol{k}) = \frac{1}{\sqrt{2\omega_{\eta'}}} \, a_i^{\eta'}(\boldsymbol{k}) \, e^{i\boldsymbol{k}\cdot\boldsymbol{r}_i} \ , \tag{8}$$

where g_{Mqq} and $g_{\eta' qq}$ are the meson-quark coupling constants for the flavor-octet and flavor-singlet mesons, respectively; $\boldsymbol{\sigma}_i$, $\boldsymbol{\lambda}_i$, and $\overrightarrow{\boldsymbol{p}}_i$ ($\overleftarrow{\boldsymbol{p}}_i$) are the spin SU(2) operator, the flavor SU(3) operator, and the initial (final) momentum operator of the ith quark, respectively. The flavor-octet meson field with the momentum $\boldsymbol{k} = \overleftarrow{\boldsymbol{p}}_i - \overrightarrow{\boldsymbol{p}}_i$ is represented by $\boldsymbol{\phi}_i(\boldsymbol{k})$ with the meson annihilation operators on the ith quark $\boldsymbol{a}_i(\boldsymbol{k})$. The flavor-singlet meson field is similarly denoted by $\phi_i^{\eta'}(\boldsymbol{k})$. The phenomenological form factor $\rho(\boldsymbol{k})$ is included to incorporate the finite size of the meson and the constituent quark.

The pseudovector coupling is one of the lowest-order terms with respect to the derivative operator of the meson field in the effective theory based on chiral symmetry [16]. This type of coupling has the favorable properties to reproduce the low-energy πN phase shift and the η production cross section around the ηN threshold [10, 17]. Note also that the pseudovector coupling brings about the same OMEP between quarks as the pseudoscalar coupling.

As mentioned above, meson-baryon continuum states have to be considered due to the meson-quark coupling H_I, in addition to the single baryon described as a three-quark bound state. Multi-meson contributions are simply neglected in this work since two-body decay channels, which are open for any nucleon resonances, often play an important role for the dynamical

properties of these resonances. We know, however, that multi-meson contributions have relatively large effects to the several partial waves such as P_{11}. We leave the calculations including the many-body contributions as a future subject.

Only π and η are considered for the flavor-octet mesons since nucleon resonances are dealt with in this paper. As in Ref. [5], η' is also taken into account. The observed values are used for the meson masses. The flavor symmetry is now broken. It therefore should be understood that the coupling constant and the energy are properly taken for each component in Eq. (5), although it is expressed in the flavor symmetric form. The model then contains three meson-quark coupling constants, $g_{\pi qq}$, $g_{\eta qq}$, and $g_{\eta' qq}$.

The mass operator for the single baryon $H_{\rm eff}(E)$ can be derived from the model Hamiltonian (1) by using the projection operator method [10]. The contribution of meson-baryon continuum states is included in the energy-dependent effective potential $W(E)$. The mass operator is written as

$$H_{\rm eff}(E) = T_0 + V_{\rm conf} + W(E) + M_0 \ , \tag{9}$$

with

$$\begin{aligned} W(E) &= H_I \frac{1}{E - H_{MB} + i\epsilon} H_I^\dagger \\ &\equiv H_I G(E) H_I^\dagger \equiv \sum_{i,j} H_I(i) G(E) H_I^\dagger(j) \ , \end{aligned} \tag{10}$$

where $H_{MB}(= H - H_I)$ is the total energy of intermediate meson-baryon states.

Because the energy-dependent effective potential $W(E)$ diverges if an infinite number of intermediate continuum states are rigorously taken into account, a prescription has to be introduced in order to perform the actual calculation [13, 18, 19]. At first, the following operators are defined as

$$\bar{G} = -\frac{1}{\omega_M} \ , \tag{11}$$

$$\begin{aligned} \bar{H}_I &= -\sum_{i=1}^{3} \frac{1}{2m}\, \rho(\boldsymbol{k})\, \boldsymbol{\sigma}_i \cdot \boldsymbol{k} \\ &\quad \times \left(g_{Mqq}\, \boldsymbol{\lambda}_i \cdot \boldsymbol{\phi}_i(\boldsymbol{k}) + \sqrt{\frac{2}{3}} g_{\eta' qq}\, \phi_i^{\eta'}(\boldsymbol{k}) \right) \\ &\equiv \sum_{i=1}^{3} \bar{H}_I(i) \ . \end{aligned} \tag{12}$$

The operators $\bar{G}$ and $\bar{H}_I$ are obtained by applying the static approximation to $G(E)$ and H_I, respectively. In this approximation, the baryons have the same energy in the initial, final, and intermediate states. By using these auxiliary operators, the effective potential $W(E)$ can be decomposed into several parts as follows:

$$\begin{aligned} W(E) &= \sum_{i,j} H_I(i) G(E) H_I^\dagger(j) - \sum_{i,j} \bar{H}_I(i) \bar{G} \bar{H}_I^\dagger(j) \\ &\quad + \sum_{i,j} \bar{H}_I(i) \bar{G} \bar{H}_I^\dagger(j) \end{aligned}$$

$$
\begin{aligned}
&= \sum_{i\neq j} \bar{H}_I(i)\bar{G}\bar{H}_I^\dagger(j) + \sum_{i,j} H_I(i)G(E)H_I^\dagger(j) \\
&\quad - \sum_{i,j} \bar{H}_I(i)\bar{G}\bar{H}_I^\dagger(j) + \sum_{i=j} \bar{H}_I(i)\bar{G}\bar{H}_I^\dagger(j) \\
&\equiv H_{\mathrm{OMEP}} + \Sigma(E) - \bar{\Sigma} + \bar{M}_0 \ .
\end{aligned} \tag{13}
$$

It can be easily shown that H_{OMEP} corresponds to the OMEP by the explicit calculation:

$$
\begin{aligned}
&H_{\mathrm{OMEP}} \\
&= \sum_{i<j} \left(\boldsymbol{\tau}_i \cdot \boldsymbol{\tau}_j V_\pi(r_{ij}) + \frac{1}{3} V_\eta(r_{ij}) + \frac{2}{3} V_{\eta'}(r_{ij}) \right) \ ,
\end{aligned} \tag{14}
$$

with

$$
\begin{aligned}
V_M(r_{ij}) &= \frac{g_{Mqq}^2}{4\pi} \frac{1}{4m^2} \frac{1}{3} \left[S_M(r_{ij}) \boldsymbol{\sigma}_i \cdot \boldsymbol{\sigma}_j \right. \\
&\quad \left. + T_M(r_{ij}) \left(\frac{3(\boldsymbol{\sigma}_i \cdot \boldsymbol{r}_{ij})(\boldsymbol{\sigma}_j \cdot \boldsymbol{r}_{ij})}{r_{ij}^2} - \boldsymbol{\sigma}_i \cdot \boldsymbol{\sigma}_j \right) \right] \ ,
\end{aligned} \tag{15}
$$

where r_{ij} is the relative separation between the ith and jth quarks, and $\boldsymbol{\tau}$ the isospin operator of quarks. The space part of the spin-spin and tensor interactions of the OMEP are denoted by S_M and T_M, respectively. They are explicitly written as follows:

$$
\begin{aligned}
S_M(r_{ij}) &= \frac{2m_M^2}{\pi} \int_0^\infty dq \frac{q^2}{q^2 + m_M^2} \rho^2(q) j_0(q r_{ij}) \\
&\quad - \frac{4}{\sqrt{\pi}} a^3 e^{-a^2 r_{ij}^2} \ ,
\end{aligned} \tag{16}
$$

$$
T_M(r_{ij}) = \frac{2}{\pi} \int_0^\infty dq \frac{q^4}{q^2 + m_M^2} \rho^2(q) j_2(q r_{ij}) \ . \tag{17}
$$

The second term of S_M, which stems from the δ-function and is properly normalized, provides short-range interactions (see Eqs. (refeqn:hamiltonian1) and (4) in Ref. [5]). The OMEP, a part of the static contributions of the effective potential $W(E)$, is free from divergence although it includes all the intermediate states. By specifying the contribution of the OMEP in $W(E)$, it becomes easy to clarify the correspondence between the present model and the conventional static models including the OMEP only [5].

The second and third terms in Eq. (13) are the self-energy $\Sigma(E)$ and the subtraction term $\bar{\Sigma}$, respectively. The subtraction term plays a crucial role to get rid of double counting, which otherwise should become a serious problem. In order to avoid the divergence in the mass operator $H_{\mathrm{eff}}(E)$, the cut-off of the intermediate states in these terms are introduced. In the present work, only πN and ηN states are taken into account because they are expected to have the largest contributions among the meson-baryon continuum states. The energy-dependence of the self-energy is quite important to reproduce the dynamical properties of baryons [10, 11, 12], while there is no energy-dependent quantity in the conventional models that contain the OMEP or the OGEP only. The $\eta' N$ state, whose threshold is near 2000 MeV, is not included since the

resulting self-energy does not have strong energy-dependence in the energy region that we are concerned with.

The matrix element of the self-energy $\Sigma^{\pi N}_{ij}(E)$, which comes from the πN intermediate state, is explicitly written as follows:

$$\Sigma^{\pi N}_{ij}(E) = \int \frac{d^3k}{(2\pi)^3} \frac{\langle N^*_i|H_I|\pi N;\boldsymbol{k}\rangle\langle \pi N;\boldsymbol{k}|H_I^\dagger|N^*_j\rangle}{E-\sqrt{m_\pi^2+k^2}-\sqrt{m_N^2+k^2}+i\epsilon}\ , \tag{18}$$

where $|\pi N;\boldsymbol{k}\rangle$ is the πN scattering state with the relative momentum $\boldsymbol{k}$. The spin-flavor dependence of the self-energy is the same as that of the OMEP since it essentially comes from the vertex function $\langle N^*|H_I|\pi N\rangle$, i.e., the matrix element of the meson-quark coupling. It has been indicated that this spin-flavor structure is important to resolve some long-standing problems in baryon spectroscopy [4]. In the integrand of Eq. (18), the relativistic form of H_{MB} is used to avoid the unphysical momentum-dependence that the non-relativistic form has in the virtual high-momentum region. For the nucleon mass, which should be calculated by the present model, the observed value is temporarily used. This is important to obtain the correct energy-dependence of the self-energy. The '$0\hbar\omega$' harmonic-oscillator wave function is used for the nucleon in the intermediate states. It has been found by numerical calculations that 90 % of the three-quark component of the nucleon consists of this '$0\hbar\omega$' wave function (see Section 3).

The state-independent divergent quantity $\bar{M}_0$ should not affect the results and it should be cancelled by some counter term. It is therefore considered in this work that the finite contribution of $\bar{M}_0$ is included in the bare mass M_0, and this quantity is removed from the potential.

Finally the mass operator is written as

$$\begin{aligned} H_{\rm eff}(E) &= T_0 + V_{\rm conf} + H_{\rm OMEP} + \Sigma^{\pi N}(E) - \bar{\Sigma}^{\pi N} \\ &\quad + \Sigma^{\eta N}(E) - \bar{\Sigma}^{\eta N} + M_0\ . \end{aligned} \tag{19}$$

It should be emphasized that the decomposition of $W(E)$ does not lead to a simple sum of the OMEP and the self-energy. In order to deal with meson-quark coupling consistently and to avoid double counting, it is necessary to include the subtraction term $\bar{\Sigma}$.

Before closing this section, we present the method of calculating the baryon mass spectrum. The matrix elements of the mass operator $H_{\rm eff}(E)$ are systematically calculated with the basis functions, i.e., the three-quark bound-state wave functions, which are the antisymmetrized products of the quark wave functions that consist of the space, spin, flavor and color parts. The spin, flavor and color wave functions are easily constructed and have well-defined symmetries. For the space part, the harmonic-oscillator wave functions are used with the range parameter β. These functions are convenient because they have analytic form and also because the c.m. motion can be easily removed by using Jacobi coordinates. The antisymmetrization can be done by using Talmi-Moshinsky coefficients [20, 21, 22].

The basis functions have to be truncated in practical applications. In the present case, the truncation requires the optimum choice of the parameter β, which determines the extension of wave functions. The most appropriate value is searched by minimizing the energy eigenvalues of the static part of $H_{\rm eff}(E)$, i.e., $T_0 + V_{\rm conf} + H_{\rm OMEP} + M_0$. The obtained value depends on the

model parameters, especially on the strength of the confinement potential. For the parameters given in table 1 in the next section, this variational method provides the value of $\beta = 3.7\,\mathrm{fm}^{-2}$. It also has been found that the basis functions upto the $8\hbar\omega$-shell of the harmonic-oscillator wave functions are enough to obtain the results with good accuracy and stability.

The energy-dependence and the imaginary part of the mass operator $H_{\rm eff}(E)$ prevent us from naively interpreting its eigenvalues as resonance masses. The resonances correspond to the S-channel poles of the propagator for meson-baryon scattering:

$$\hat{G} \propto \frac{1}{E - H_{\rm eff}(E)} \ . \tag{20}$$

Therefore the resonance mass E_R can be approximately determined as the solution of

$$\mathrm{Re}(E_R - H_{\rm eff}(E_R)) = 0 \ , \tag{21}$$

after the energy-dependent eigenvalues are obtained by the diagonalization of the mass operator $H_{\rm eff}(E)$.

3 Results and discussions

The present model still has six parameters to be determined: the strength of the confinement potential c, the form factor parameter a, the bare mass of baryons M_0, and the π-, η-, and η'-quark coupling constants, $g_{\pi qq}$, $g_{\eta qq}$, and $g_{\eta' qq}$, respectively. The parameters except $g_{\pi qq}$ are phenomenologically determined to reproduce the prominent feature of the mass spectrum of the spin $\frac{1}{2}$ nucleon resonances: The separations among the negative- and positive-parity resonances are relatively small in comparison with the large mass difference between the ground state nucleon and the other resonances. All the parameters thus determined are summarized in table 1.

The π-quark coupling constant $g_{\pi qq}$ is derived from the πN coupling constants $G_{\pi NN}$ by using the spin-flavor SU(6) relation of the quark model. The standard value of $G_{\pi NN}$ cited in Ref. [23] is used: $G_{\pi NN} = 14.3$. For the determination of the η- and η'-quark coupling constants, $g_{\eta qq}$ and $g_{\eta' qq}$, the observed values of the meson-nucleon coupling constants are not used because of the badly broken flavor SU(3) relation for these mesons. For $g_{\eta qq}$, for example, the fitting process provides the small value of 3.52, which is different from the value of 4.59 derived from the η-nucleon coupling constant.

The excitation energies put the constraint on the determination of the confinement strength c. Because Eq. (21) is a non-linear equation of energy variable, the role of M_0 is more than just an additional constant. The phenomenological parameter a, which may be related with the finite size of the meson and the constituent quark, is quite difficult to be determined from other sources of information. In the fitting procedure, this parameter has correlation with the meson-quark coupling strengths through the momentum dependence of the form factor.

Let us present the mass spectra of the current model. The masses of the spin $\frac{1}{2}$ nucleon resonances are shown in Fig. 1. The calculation can reproduce the general feature of the observed spectrum fairly well. The excitation energies of the first negative-parity states are calculated to be about 500 MeV, and the mass differences among the excited nucleons becomes relatively small compared with the excitation energies.

In order to make clear the reason why the model can reproduce these features, each contribution of the mesonic effects on the mass spectrum is examined. As is seen in Fig. 1, where the result without the self-energy $\Sigma(E)$ and subtraction term $\bar{\Sigma}$ is also shown, the self-energy, as well as the OMEP, significantly contributes to the mass spectrum. In the consistent treatment of the meson-quark coupling in this work, the self-energy has almost the same magnitude as the OMEP. For example, the diagonal element of the OMEP for the ground-state nucleon is $-175\,\mathrm{MeV}$, and the corresponding self-energy $\Sigma(E \simeq m_N)$ is about $-400\,\mathrm{MeV}$. The subtraction term $\bar{\Sigma}$ is $-266\,\mathrm{MeV}$, and is comparable with the self-energy and the OMEP. Therefore the naive sum of the self-energy and the OMEP without this subtraction causes serious overestimate of the mesonic effects. It should be also emphasized that the subtraction term depends on the initial and final baryon states and is not merely a constant parameter.

For the positive-parity states, Fig. 2 shows that the self-energy due to the ηN state is generally smaller than that due to the πN state. This is because of the restriction of the phase space since the ηN threshold is higher than the πN threshold. The self-energy for the ground-state nucleon N is remarkably large because N strongly couples to the intermediate πN state without changing the configuration of quarks in a baryon. The nucleon mass is pulled down partly owing to this effect.

In Fig. 3, the cusp behavior is seen at the ηN threshold for the negative-parity states due to their S-wave coupling to the ηN state. It is a characteristic feature of the self-energy, and this energy dependence is important to the dynamical properties of resonances. The OMEP does not have such energy-dependence.

For the states in the same '$\hbar\omega$'-shell, the non-diagonal elements of the self-energy have the same magnitude as the diagonal elements. Note, however, that the state mixing among the different shells is relatively small since the off-diagonal elements of the total mass operator $H_{\mathrm{eff}}(E)$ are in general smaller than the differences in its diagonal elements.

In the present calculation, the mass of the ground-state nucleon N is $1017\,\mathrm{MeV}$, which is larger than the observed one by about $10\,\%$. The disagreement is partly ascribed to the approximate treatment of N in the intermediate πN and ηN states. In these decay channels, N is considered just a three-quark bound state since multi-meson states are neglected in this work. The physical nucleon is, however, the admixture of the three-quark state, meson and three-quark state, and so on. The probability of observing the three-quark component is related with the energy-derivative of $\Sigma(E)$ as

$$Z^{-1} = 1 - \mathrm{Re}\left(\frac{\mathrm{d}}{\mathrm{dE}}\Sigma^{\pi\mathrm{N}}(\mathrm{E}) + \frac{\mathrm{d}}{\mathrm{dE}}\Sigma^{\eta\mathrm{N}}(\mathrm{E})\right)_{\mathrm{E}=\mathrm{E_R}} . \tag{22}$$

Due to the strong energy-dependence of $\Sigma(E)$ around E_R, the probability Z deviates from 1: We obtain $Z \simeq 0.6$ for N. Because the relatively large part of the wave function is occupied by the meson-nucleon component, further study of the mesonic effects is required if we try to describe the property of the nucleon in detail.

We examine the role of the spin-flavor symmetry of the OMEP by comparing it with the "color-spin symmetry" of the OGEP. To show the difference between the OMEP and the OGEP in an explicit way, we consider the $\frac{1}{2}^+$ and $\frac{1}{2}^-$ excited-states, which are $2\hbar\omega$ and $1\hbar\omega$ excited-states, respectively. The three-quark bound-state with $[3]_{\mathrm{space}} \otimes [21]_{\mathrm{spin}} \otimes [21]_{\mathrm{flavor}} \otimes [111]_{\mathrm{color}}$ symmetry is taken for the $\frac{1}{2}^+$ state, and that with $[21]_{\mathrm{space}} \otimes [21]_{\mathrm{spin}} \otimes [21]_{\mathrm{flavor}} \otimes [111]_{\mathrm{color}}$

symmetry is taken for the $\frac{1}{2}^-$ state. Note that $N(1440)$ is dominated by this $\frac{1}{2}^+$ state. On the other hand, the symmetry property of the OMEP is characterized by $f\boldsymbol{\lambda}_i \cdot \boldsymbol{\lambda}_j \boldsymbol{\sigma}_i \cdot \boldsymbol{\sigma}_j$, where f stands for the spatial part of the interaction, and i and j denote the i th and j th quarks, respectively. Similarly, the OGEP has the operator $-g\,\boldsymbol{\sigma}_i \cdot \boldsymbol{\sigma}_j$. We obtain the diagonal matrix elements of these operators as shown in table 2. Since these potentials are of short-range and attractive, the following relations hold: $\langle f\rangle_{00} < \langle f\rangle_{10} < \langle f\rangle_{01} < 0$ and $\langle g\rangle_{00} < \langle g\rangle_{10} < \langle g\rangle_{01} < 0$. In the case of the OMEP, the difference is $\frac{5}{2}\langle f\rangle_{10} + \frac{3}{5}\langle f\rangle_{01}$. Since the two terms are added constructively, the mass of the $\frac{1}{2}^+$ state is lowered more largely than that of the $\frac{1}{2}^-$ state due to the OMEP, that is, the former gets close to the latter. In the case of the OGEP, on the other hand, the difference is $\frac{1}{2}(\langle g\rangle_{10} - \langle g\rangle_{01})$, the magnitude of which becomes small owing to the destructive combination. The similar argument can be applied to the other $\frac{1}{2}^-$ state with $[21]_{\rm space} \otimes [3]_{\rm spin} \otimes [21]_{\rm flavor} \otimes [111]_{\rm color}$ symmetry. The property of the spin-flavor symmetry in the OMEP is thus consistent with the fact the observed mass of $N(1440)$ is remarkably light.

The spin-flavor symmetry of the self-energy also plays an important role in making the $\frac{1}{2}^+$ resonances come close to the $\frac{1}{2}^-$ resonances, as is shown in Fig. 1. The symmetry structure of the meson-quark coupling is characterized by the operator $\boldsymbol{\sigma}_i\,\boldsymbol{\lambda}_i$ (see Eq. (5)). Taking the same states (see table 2) for examples, we obtain the ratio of the spin-flavor parts of the $\pi N N^*$ vertices as

$$\frac{5\sqrt{2}}{4} = \frac{\frac{1}{2}^+ \to \pi N \text{transition}}{\frac{1}{2}^- \to \pi N \text{transition}} \,. \tag{23}$$

The ratio for the other $\frac{1}{2}^-$ state with $[21]_{\rm space} \otimes [3]_{\rm spin} \otimes [21]_{\rm flavor} \otimes [111]_{\rm color}$ is $5\sqrt{2}/2$ for spin-nonflip transition. We can therefore expect that the mass shift of $N(1440)$ is larger than that of $N(1535)$ (see Eq. (18)). More quantitative discussion needs proper treatment of the space part in each matrix element of the self-energy. The numerical calculations show that these mass shifts are also attractive and the spin-flavor symmetry of the self-energy is important to reproduce the nucleon mass spectrum.

In spite of the favorable property of the spin-flavor symmetry in the present model, $N(1440)$ still locates above the negative-parity resonances although it is experimentally observed below them. Glozman *et al.* have recently claimed that their OMEP model reproduces the mass of $N(1440)$ if the relativistic kinematics is used for quarks [6]. (Although they can explain the mass spectrum with the non-relativistic kinematics in their first paper [5], the δ-function part of the OMEP, i.e., the second term of Eq. (16), has an artificially large strength.) If the relativistic correction in the kinetic energy operator is so important, the vertex functions should be also modified in a consistent manner. We leave such a calculation with relativistic corrections as a future project.

We proceed to show the spectra of the spin $\frac{3}{2}$ and $\frac{5}{2}$ nucleon resonances in Fig. 4. All the parameters for these resonances are the same as those for the spin $\frac{1}{2}$ resonances. The calculated masses of these resonances roughly agree with the observed values although the mass differences between the positive- and negative-parity states are too large. It should be noticed that the common bare mass M_0 can be used for all the nucleon resonances. The form factor $\rho(\boldsymbol{k})$ plays an important role in this success. For example, the lowest $\frac{1}{2}^-$ and $\frac{3}{2}^-$ resonances, i.e., $N(1535)$ and $N(1520)$, are considered. If $\rho(\boldsymbol{k})$ is removed from the calculation of the self-energy, the mass of $N(1520)$ becomes smaller by about 60 MeV, while that of $N(1535)$ changes by a few MeV only. This is because the D-wave $\pi N N(1520)$ coupling has large high-momentum component

than the S-wave $\pi NN(1535)$ coupling. The effect of $\rho(\boldsymbol{k})$ is favorable since it reduces the contribution from the virtual high-energy intermediate states that the present model may not be applied to. But for $\rho(\boldsymbol{k})$, the spin-dependence of M_0 should be inevitable.

4 Summary

We have constructed the constituent quark model which contains the meson-quark coupling to incorporate the spontaneous breaking of chiral symmetry in low-energy QCD, and calculated the masses of nucleon resonances. The meson-quark coupling has the spin-flavor dependence which is thought to be important for the low-energy baryon spectrum. In the present formalism, the consistent treatment of the meson-quark coupling provides the OMEP and the self-energy of baryons with the subtraction term, which is important to avoid the problem of double counting. Since both of the mesonic effects are significantly large, we should take account of these terms simultaneously if we try to include the mesonic effects in the model of baryons. The results show that the model reproduces the gross feature of the observed mass spectra, whereas the mass of $N(1440)$ is still too high.

In order to refine the calculations, we have to include not only the πN and ηN states but also the states that contain other mesons and baryons, such as $\pi\Delta$ and ρN. These states, which are closely related to the $\pi\pi N$ channel, are considered to be important for the detailed study of nucleon resonance spectroscopy. Relativistic corrections are to be investigated in near future also.

Furthermore, we have to calculate the scattering quantities and compare them directly with the experimental data in order to complete the investigation of the model. This type of study is necessary since the masses of nucleon resonances represent only a small part of the information of the phase shift analysis of the πN scattering. The calculation of the scattering quantities are now in progress. On the other hand, it is also desirable to study strange baryons in this model, and the results will be shown elsewhere.

Acknowledgements

We would like to thank Prof. R. Seki for valuable suggestions and discussions. We are much indebted to Prof. T. Sato and Dr. T. Ogaito for discussions on the method of calculation. One of the authors (H.K.) would like to thank Prof. Y. Kudo and Prof. Y. Sakuragi for their continuous encouragement.

References

[1] A. J. G. Hey and R. L. Kelly, Phys. Rep. **96**, 71 (1983).

[2] N. Isgur and G. Karl, Phys. Rev. **D18**, 4187 (1978); N. Isgur and G. Karl, Phys. Rev. **D19**, 2653 (1979); N. Isgur and G. Karl, Phys. Rev. **D20**, 1191 (1979).

[3] Particle Data Group, Phys. Rev. **D54**, 1 (1996).

[4] L. Ya Glozman and D. O. Riska, Phys. Rep. **268**, 263 (1996).

[5] L. Ya. Glozman, Z. Papp, and W. Plessas, Phys. Lett. **B381**, 311 (1996).

[6] L. Ya. Glozman, W. Plessas, K. Varga, and R. F. Wagenbrunn, hep-ph/9706507.

[7] A. De Rújula, H. Georgi, and S. L. Glashow, Phys. Rev. **D12**, 147 (1975).

[8] A. Manohar and H. Gerogi, Nucl. Phys. **B234**, 189 (1984).

[9] T. P. Cheng and L. F. Li, Phys. Rev. Lett. **74**, 2872 (1995).

[10] M. Arima, K. Shimizu, and K. Yazaki, Nucl. Phys. **A543**, 613 (1992).

[11] T. Hamaie, M. Arima, and K. Masutani, Nucl. Phys. **A591**, 675 (1995).

[12] T. Hamaie, K. Masutani, and M. Arima, Nucl. Phys. **A607**, 363 (1996).

[13] S. A. Chin, Nucl. Phys. **A382**, 355 (1982).

[14] M. Creutz, *Quarks, Gluons and Lattices* (Cambridge University Press, Cambridge, 1983), pp.54.

[15] J. Kogut and L. Susskind, Phys. Rev. **D9**, 3501 (1974).

[16] D. K. Campbell, in *Les Houches 1977 Nuclear Physics with Heavy Ions and Mesons* vol.2 (North-Holland, Amsterdam, 1978), pp.622.

[17] H. A. Bethe and F. de Hoffmann, *Mesons and Fields* (Row, Peterson & Company, Evanston, 1955).

[18] E. Oset, Nucl. Phys. **A411**, 357 (1983).

[19] K. G. Horacsek, Y. Iwamura, and Y. Nogami, Phys. Rev. **D32**, 3001 (1985).

[20] T. Ogaito and T. Sato, private communication

[21] Yu. F. Smirnov, Nucl. Phys. **27**, 177 (1961).

[22] L. Trlifaj, Phys. Rev. **C5**, 1534 (1972).

[23] G. C. Oades, H. Behrens, J. J. de Swart, and P. Kroll, Nucl. Phys. **B216**, 277 (1983).

Table 1: The values of the parameters. The other parameters used in the calculations are as follows: $m = 340\,\mathrm{MeV}$, $\beta = 3.7\,\mathrm{fm}^{-2}$, and the observed values are used for the meson masses.

$c\,(\mathrm{fm}^{-2})$	$a\,(\mathrm{fm}^{-1})$	$g_{\pi qq}$	$g_{\eta qq}$	$g_{\eta' qq}$	M_0 (MeV)
1.5	2.5	2.91 (fixed)	3.52	3.23	0

Table 2: The matrix elements of the OMEP and the OGEP for $\frac{1}{2}^+$ and $\frac{1}{2}^-$ resonances. The spatial matrix elements for the state with the node n and the angular momentum l are denoted by $\langle f\rangle_{nl}$ and $\langle g\rangle_{nl}$.

J^π	OMEP	OGEP
$\frac{1}{2}^+$	$\frac{5}{2}(\langle f\rangle_{00} + \langle f\rangle_{10})$	$\frac{1}{2}(\langle g\rangle_{00} + \langle g\rangle_{10})$
$\frac{1}{2}^-$	$\frac{5}{2}(\langle f\rangle_{00} - \frac{3}{5}\langle f\rangle_{01})$	$\frac{1}{2}(\langle g\rangle_{00} + \langle g\rangle_{01})$

Figure 1: The mass spectrum of nucleon resonances with spin $\frac{1}{2}$. The calculations are compared with the experimental data. The corresponding states are connected by dashed lines. The contributions of H_{OMEP}, $\Sigma(E)$, and $\bar{\Sigma}$ are examined also. (a) The data taken from the particle data table [3]. The parities of the resonances are shown. (b) The result of the present model. (c) The result without $\Sigma(E)$ and $\bar{\Sigma}$. (d) The result without H_{OMEP}, $\Sigma(E)$, and $\bar{\Sigma}$.

Figure 2: (a) The matrix elements of $\Sigma^{\pi N}(E) - \bar{\Sigma}^{\pi N}$ for the positive-parity nucleon resonances with spin $\frac{1}{2}$. The solid line corresponds to the diagonal element of the $0\hbar\omega$ state, and the dashed line to that of the $2\hbar\omega$ state. Among the diagonal elements of the four $2\hbar\omega$ states, only the largest one is shown here. (b) Same as (a) but for $\Sigma^{\eta N}(E) - \bar{\Sigma}^{\eta N}$.

Figure 3: Same as Fig. 2 but for the negative-parity nucleon resonances with spin $\frac{1}{2}$. The diagonal elements and the nondiagonal element for the two $1\hbar\omega$ states are shown. The solid line corresponds to the diagonal element of the intrinsic-spin $\frac{3}{2}$ state, the dashed line to that of the intrinsic-spin $\frac{1}{2}$ state, and the dot-dashed line to the nondiagonal element between these states. Because the $\eta N N^*$ vertices for these negative-parity states are identical, all the matrix elements for the ηN coupling have the same value, that is, the three lines coincide with each other.

Figure 4: The numerical results are compared with the observed spectra of nucleon resonances with spin $\frac{1}{2}$ (left), $\frac{3}{2}$ (center), and $\frac{5}{2}$ (right). The dashed lines represent the correspondence between the calculations and the data. The parities of the states are also shown.

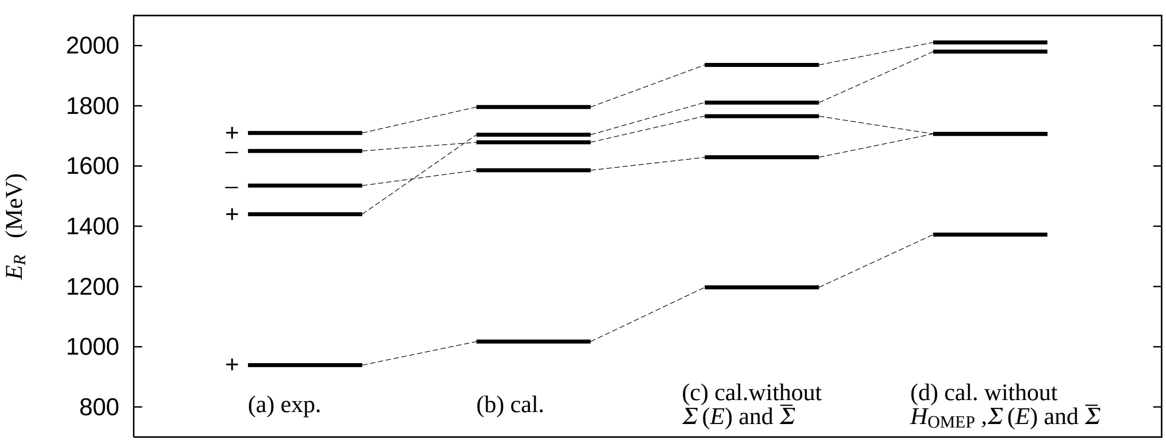

E_R (MeV)
2000
1800
1600
1400
1200
1000
800
+
−
−
+
+
(a) exp.
(b) cal.
(c) cal.without $\Sigma(E)$ and $\overline{\Sigma}$
(d) cal. without $H_{\rm OMEP}$,$\Sigma(E)$ and $\overline{\Sigma}$

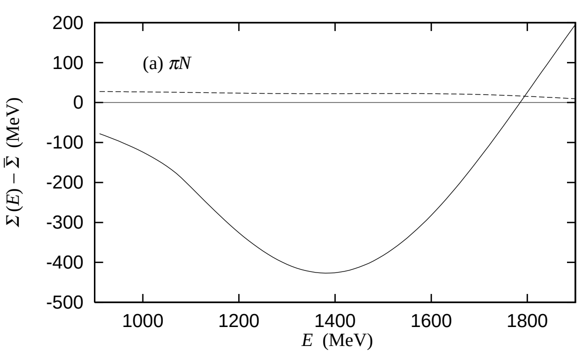

(a) πN
$\Sigma(E) - \bar{\Sigma}$ (MeV)
200
100
0
-100
-200
-300
-400
-500
1000
1200
1400
1600
1800
E (MeV)

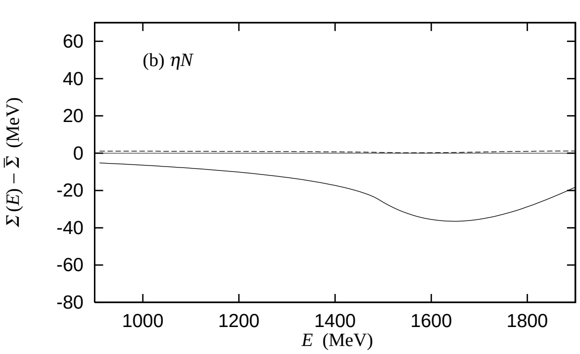

(b) ηN
$\Sigma(E) - \bar{\Sigma}$ (MeV)
60
40
20
0
-20
-40
-60
-80
1000
1200
1400
1600
1800
E (MeV)

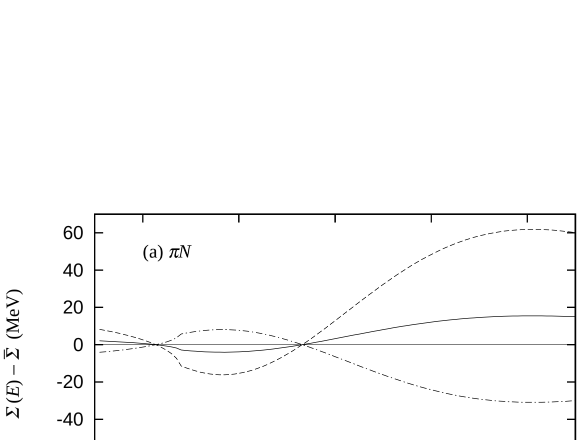

(a) πN
60
40
20
0
-20
-40
-60
-80
1000
1200
1400
1600
1800
E (MeV)
$\Sigma(E) - \bar{\Sigma}$ (MeV)

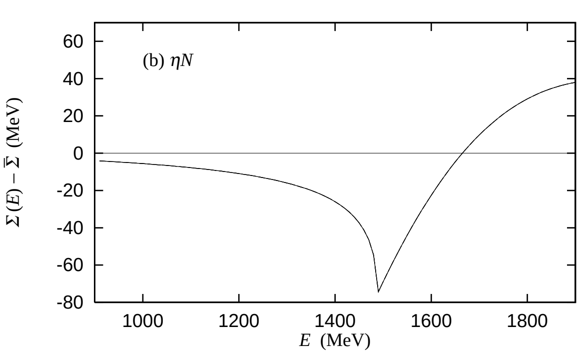

(b) ηN
60
40
20
0
-20
-40
-60
-80
1000
1200
1400
1600
1800
E (MeV)
$\Sigma(E) - \bar{\Sigma}$ (MeV)

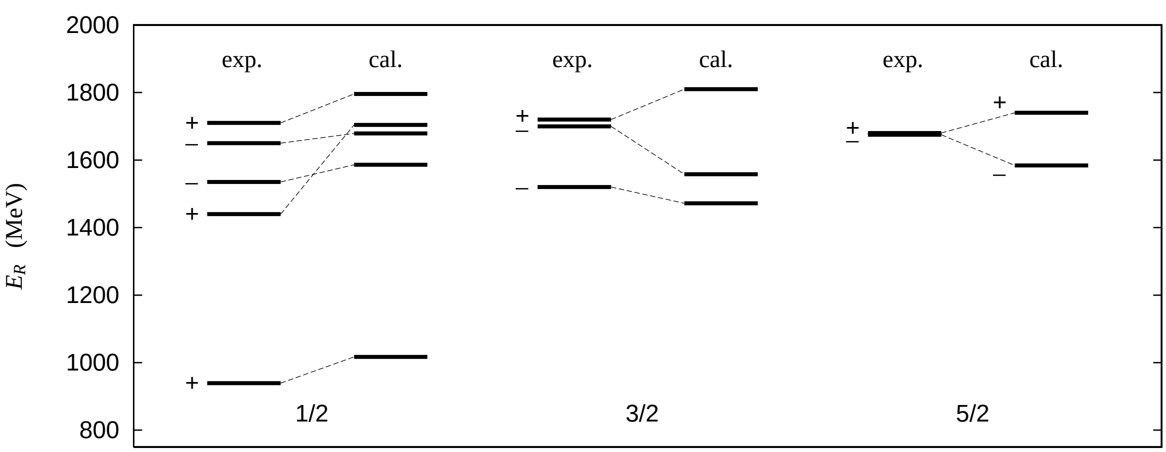

2000
1800
1600
1400
1200
1000
800
E_R (MeV)
exp.
cal.
exp.
cal.
exp.
cal.
+
−
−
+
+
+
−
−
+
−
+
−
1/2
3/2
5/2